Synthesis, characterization and bromination of bis(phosphinoferrocenyl) gold(I) compounds

Tebogo V. Segapelo [a], Ilia A. Guzei [b], James Darkwa [a,*]

[a] *Department of Chemistry, University of Johannesburg, Auckland Park Kingsway Campus, P.O. Box 524, Johannesburg 2006, South Africa*
[b] *Department of Chemistry, University of Wisconsin-Madison, 1101 University Avenue, Madison, WI 53706, United States*

Abstract

Reaction of [(dppf)Au$_2$Br$_2$] (**3**) {dppf = 1,1′-bis(diphenylphosphino)ferrocene} and [(dippf)Au$_2$Br$_2$] (**4**) {dippf = 1,1′-bis (diisopropylphosphino)ferrocene} with excess bromine yields two new complexes [(C$_5$H$_4$Br$_3$)(PR$_2$)AuBr] (R = Ph, **5**; R = *i*-Pr, **6**). Bromination of the free diphosphinoferrocene ligands produces the expected brominated cyclopentenes (C$_5$H$_4$Br$_3$)(PR$_2$) (R = Ph, **7**; R = *i*-Pr, **8**) in good yields; however, these compounds could not be complexed to gold due to reduced basicity of **7** and **8**. When the bromination is performed under wet aerobic conditions the oxidized pseudo-centrosymmetric product, [doppf][FeBr$_4$] (**9**) {doppf = 1,1′-bis(oxodiphenylphosphino)ferrocene, is formed as the major product. Solid-state structures of **1**, **2**, **4**, **6**, and **9** have been established by means of single-crystal X-ray crystallography.
© 2007 Elsevier B.V. All rights reserved.

Keywords: Diphenylphosphinoferrocene; Diisopropylphosphinoferrocene; Bromination; Phosphinocyclopentene; Ligands; Gold(I) complexes

1. Introduction

Ferrocene has become a versatile building block for the synthesis of compounds with tailor-made properties. This has been made possible by well-established methods for its incorporation into complex structures [1–4]. Compounds with donor heteroatoms (e.g. P, N, S, O) substituted onto cyclopentadienyl rings dominate its chemistry especially those featuring homo-substituents. One such ligand, 1,1′-bis(diphenylphosphino)ferrocene (dppf), has been used for the past three decades due to the interesting structural and redox properties of its metal compounds [1]. The popularity of the diphosphines stems from their ability to modify their bite angle in order to adapt to different geometric requirement. In particular, group 10 metal dppf compounds are the most extensively studied [5]. For instance, we observed that dppf palladium and platinum complexes can be used to form thiolate complexes that

can absorb sulfur dioxide reversibly [6]. Ironically, dppf has fewer gold complexes reported in the literature, and only a few of these are Au(III) complexes [7].

During our attempts to prepare Au(III) complexes with dppf and its isopropyl analogue (dippf), we discovered that the Au(III) starting materials are readily reduced to Au(I) in the presence of these diphosphines. Attempts to oxidize the reduced products by bromine resulted in bromination of the cyclopentadienyl rings and subsequent demetallation of the diphenylphosphinoferrocene ligand. Herein we present the synthesis and reactivity of dppf and dippf Au(I) complexes and their reactions that led to the bromination of the cyclopentadienyl rings of dppf and dippf.
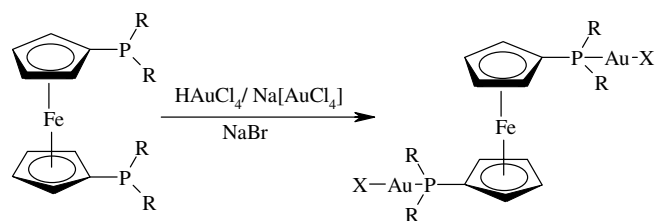
2. Results and discussion

2.1. Gold complexes of dppf and dippf

Complexes **1**–**4** were prepared from equimolar amounts of either Na[AuCl$_4$] or HAuCl$_4$ and the appropriate diphosphino ligand (Scheme 1). Syntheses of the bromo

---

* Corresponding author.
  E-mail address: jdarkwa@uj.ac.za (J. Darkwa).

R	X	Complex	Yield(%)
Ph	Cl	**1**	45
i-Pr	Cl	**2**	42
Ph	Br	**3**	16
i-Pr	Br	**4**	37

Scheme 1. Preparation of complexes **1–4**.

analogues (**3** and **4**) were performed according to the reactions in Scheme 1 in the presence of excess NaBr. The yields obtained were generally low.

Addition of excess phosphine to Au(III) is known to reduce it to Au(I) [8], hence the low yields obtained might be due to some of the diphosphinoferrocene ligands acting as a reducing agent and thus only small amounts of it are available to react with the Au(I) produced. When a twofold excess of the phosphines was used the yields improved only slightly.

Whereas the reactions in Scheme 1 using dppf and dippf with the gold starting materials produced the known complexes **1–3** [9a,9b–12], only **1** has previously been structurally characterized. In addition to spectroscopic characterization of **1–4**, single crystal X-ray determination confirmed the structures deduced from our spectroscopic data. Table 1 gives crystallographic data for **1**, **2** and **4** and Figs. 1–3 show molecular drawing diagrams and selected metric parameters for these three complexes.

Three (pseudo)polymorphs are known for **1**: unsolvated **1** [9a] and **1a** [9b], a chloroform solvate **1·2/3CHCl₃**, [10] and a bis-dichloromethane solvate **1·2CH₂Cl₂** [11]. While the interatomic bond distances and angles are similar in all four structures the mutual orientation of the substituted Cp rings is worth mentioning. The unsolvated **1**, whose structure is reported herein, crystallizes in the monoclinic space group $C2/c$ with $Z' = 0.5$ at 100 K and the complex resides on a crystallographic inversion centre. The P1–Centroid1–Centroid2–P(1A) torsion angle is 180° with the antiperiplanar arrangement and staggered the Cp rings (180°) due to the imposed symmetry. In the polymorph **1a** this angle is 162.8° and the arrangement is antiperiplanar. In pseudopolymorph **1·2/3CHCl₃** there are two symmetry independent complexes, the first one resides on a crystallographic inversion centre and exhibits features similar to those in **1**. The other molecule does not have any crystallographic symmetry and the P1–Centroid1–Centroid2–P(1A) torsion angle spans 125.3° which corresponds to an anticli-

Table 1
Crystallographic data for **1**, **2**, **4**, **6** and **9**

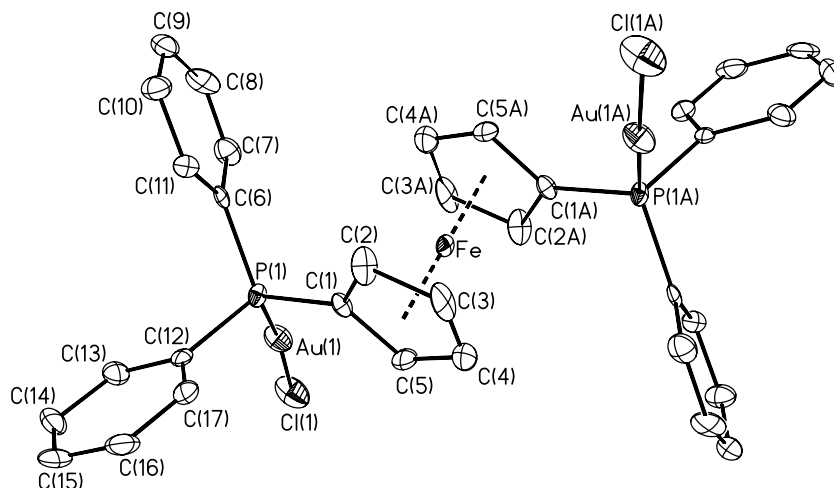|	1	2	4	6	9
Empirical formula	$C_{34}H_{28}Au_2Cl_2FeP_2$	$C_{22}H_{36}Au_2Br_2FeP_2$	$C_{22}H_{36}Au_2Cl_2FeP_2$	$C_{11}H_{18}AuBr_4P$	$C_{34}H_{29}Br_4Fe_2O_2P_2$
Formula weight	1019.19	972.05	883.13	697.83	962.85
Temperature (K)	100(2)	100(2)	100(2)	100(2)	105(2)
Wavelength (Å)	0.71073	0.71073	0.71073	0.71073	0.71073
Crystal system	Monoclinic	Monoclinic	Monoclinic	Monoclinic	Triclinic
Space group	$C2/c$	$C2/c$	$C2/c$	$P2_1/c$	$P\bar{1}$
a (Å)	15.8958(18)	25.9048(12)	25.9629(19)	13.857(2)	10.9884(7)
b (Å)	13.1673(15)	7.8665(4)	7.5672(6)	10.1413(15)	12.7674(9)
c (Å)	15.0236(17)	14.3244(7)	14.2703(11)	13.3486(19)	13.6125(9)
α (°)	90	90	90	90	84.4600(10)
β (°)	99.896(2)	110.7470(10)	110.3490(10)	114.928(2)	67.0920(10)
γ (°)	90	90	90	90	80.5570(10)
Volume (Å³)	3097.7(6)	2729.7(2)	2628.7(3)³	1701.1(4)	1734.2(2)
Z	4	4	4	4	2
D_{calc} (Mg/m³)	2.185	2.365	2.232	2.725	1.844
Absorption coefficient (mm⁻¹)	10.211	14.300	12.012	18.117	5.567
Crystal size (mm³)	0.41 × 0.35 × 0.33	0.37 × 0.33 × 0.24	0.45 × 0.31 × 0.16	0.24 × 0.21 × 0.12	0.28 × 0.14 × 0.14
Reflections collected	12091	10541	10394	18345	30240
Absorption correction	Multi-scan with SADABS	Multi-scan with SADABS	Multi-scan with SADABS	Multi-scan with SADABS	Empirical with SADABS
Maximum and minimum transmission	0.1336 and 0.1024	0.1307 and 0.0765	0.2495 and 0.0745	0.2198 and 0.0977	0.5095 and 0.3047
Goodness-of-fit on F^2	1.17	1.137	1.082	1.094	0.996
Final R indices [$I > 2\sigma(I)$]	$R_1 = 0.0762$, $wR_2 = 0.2031$	$R_1 = 0.0168$, $wR_2 = 0.0414$	$R_1 = 0.0149$, $wR_2 = 0.0369$	$R_1 = 0.0357$, $wR_2 = 0.0953$	$R_1 = 0.0198$, $wR_2 = 0.0535$
R indices (all data)	$R_1 = 0.0819$, $wR_2 = 0.2056$	$R_1 = 0.0178$, $wR_2 = 0.0418$	$R_1 = 0.0158$, $wR_2 = 0.0373$	$R_1 = 0.0381$, $wR_2 = 0.0965$	$R_1 = 0.0222$, $wR_2 = 0.0545$

Fig. 1. Molecular drawing of **1** shown with 30% probability ellipsoids. The hydrogen atoms are omitted for clarity. Selected interatomic distances (Å) and angles (°) for **1**: Au(1)—P(1) 2.238(4); Au(1)–Cl(1) 2.254(5); P(1)–C(1) 1.777(15); P(1)–C(6) 1.819(16); P(1)–C(12) 1.816(16); and P(1)–Au(1)–Cl(1) 171.83(17).
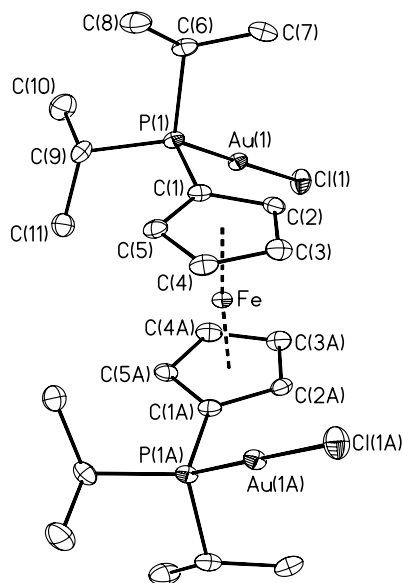

Fig. 2. Molecular drawing of **2** shown with 50% probability ellipsoids. The hydrogen atoms are omitted for clarity. Selected interatomic distances (Å) and angles (°) for **2**: Au(1)–P(1) 2.2369(6); Au(1)–Cl(1) 2.2883(6); P(1)–C(1) 1.837(3); P(1)–C(6) 1.852(3); P(1)–C(9) 1.797(3); P(1)–Au(1)–Cl(1) 178.13(2).
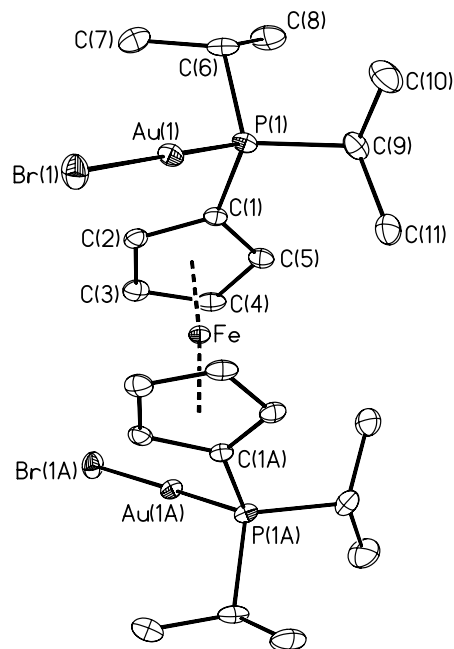

Fig. 3. Molecular drawing of **4** shown with 50% probability ellipsoids. The hydrogen atoms are omitted for clarity. Selected interatomic distances (Å) and angles (°) for **4**: Au(1)–P(1) 2.2408(7); Au(1)–X(1) 2.4031(3); P(1)–C(1) 1.794(3); P(1)–C(6) 1.853(3); P(1)–C(9) 1.842(3); P(1)–Au(1)–X(1) 176.768(19).

nal arrangement with a mutual orientation of the Cp rings intermediate between staggered (108°) and eclipsed (144°). The complex in the other solvated pseudopolymorph **1·2CH₂Cl₂** also resides on an inversion centre and the arrangement is therefore antiperiplanar staggered.

Complexes **2** and **4** also contain two linearly coordinated gold atoms bound to the diphosphinoferrocene ligand and have linear geometries around the gold atoms. The two cyclopentadienyl rings in the ferrocenyl groups are essentially eclipsed which is expected behaviour of the majority of monosubstituted ferrocenyl derivatives [13].

The P–Centroid1–Centroid2–P torsion angle in the isomorphous solid-state structures of **2** and **4** spans 147.1° corresponding to an anticlinal arrangement.

The Au-halide arrangement with phosphines are however different from **1**. In complex **1** the Au–P–P–Au torsion angle is 180.0° (antiperiplanar) due to the symmetry considerations whereas in **2** and **4** the corresponding angles span 110.3° and 112.5° (anticlinal), respectively. The Au–P and Au–Cl distances in **1** and **2** (and Au–P distance in **4** and
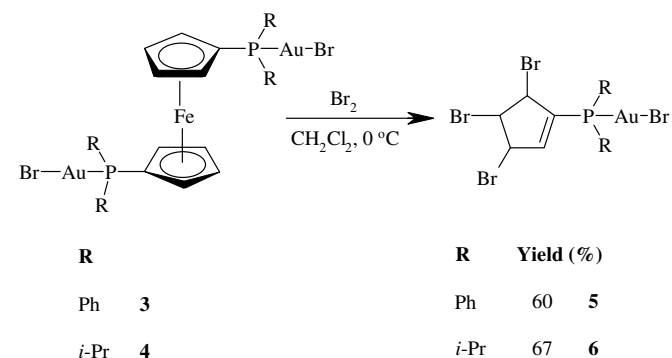
6) are in excellent agreement with the average values of 2.229(15) and 2.288(13) Å, respectively, obtained by averaging 346 relevant valued complexes reported to the Cambridge Structural Database (CSD). The Au–Br bond distances in **4** and **6** agree well with the average value of 2.404(10) Å computed for 41 relevant complexes reported to the CSD. The P–Au–Halogen angles in **1**, **2**, **4**, and **6** approach linearity as expected.

2.2. Demetallation of complexes and ligands by bromine

Of the three coinage metals, only gold is readily oxidized to the +3 oxidation state. Schneider et al. [14] have shown that when an oxidant such as bromine is added to [(dppm)(AuBr)$_2$] (dppm = diphenylphosphinomethane), it first gives [(dppm)AuBr(AuBr$_3$)] and subsequently [(dppm)(AuBr$_3$)$_2$]. In an attempt to use this approach to re-convert the Au(I) complexes **3** and **4** to Au(III), we reacted these complexes with bromine (Scheme 2). We, however, isolated complexes **5** and **6**; showing that bromination of the cyclopentadienyl rings rather than oxidation of the Au atom had occurred. Compound **5** was obtained in 64% yield as a red solid, while **6** was obtained in 44% yield as gold-coloured crystals.

In the ^{1}H NMR spectrum of **5**, peaks due to the brominated cyclopentene ring appear at 6.76, 5.77, 5.38 and 5.05 ppm, while the phenyl peaks of the diphenylphosphine appear as a multiplet centred at 7.65 ppm. The ^{1}H NMR spectrum of **6** also shows a similar chemical shift pattern with peaks due to the brominated cyclopentene ring appearing at 6.78, 5.25, 5.20, and 4.98 ppm, with the proton on the carbon of the double bond being the most downfield peak and peaks due to the isopropyl moieties appearing at approximately 2.62 and 1.56 ppm as multiplets.

The structure for complex **6** was determined by single X-ray crystallography. Crystallographic data are in Table 1 and molecular drawing diagram of **6** and bond parameters are presented in Fig. 4. The structure of **6** bears resemblance to the recently reported structure for E^1-1-(i-Pr)$_2$P-2-Me2 N-indeneAuCl complex [15]. The five-mem-
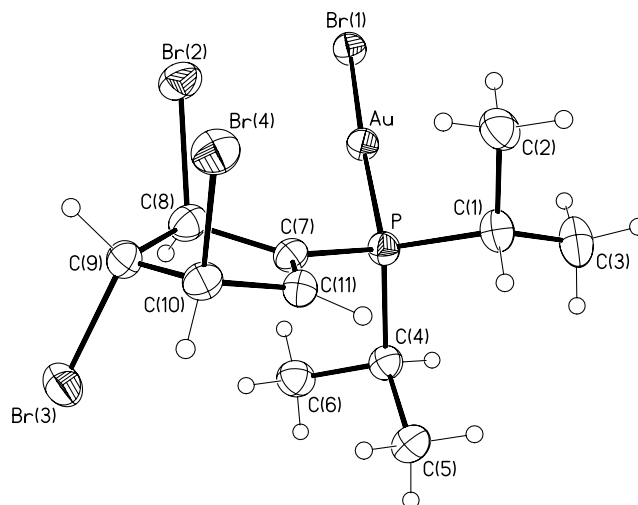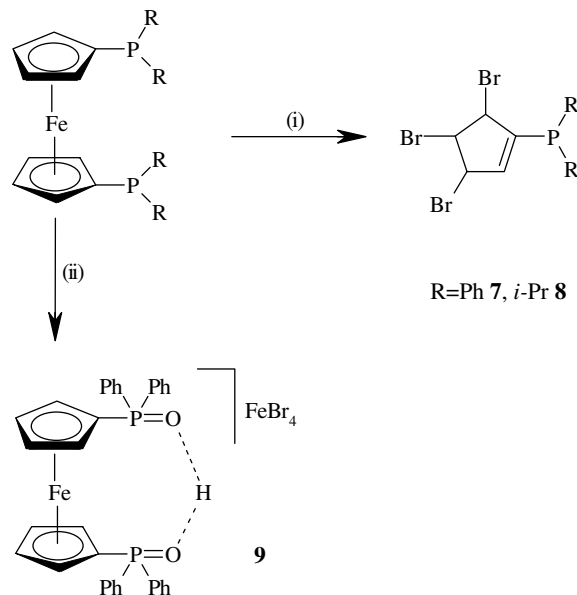

Fig. 4. Molecular drawing of **6** shown with 50% probability ellipsoids. Selected interatomic distances (Å) and angles (°) for **4**: Au–P 2.2376(16); Au–Br(1) 2.4046(7); P–C(7) 1.806(6); P–C(4) 1.840(7); P–C(1) 1.836(7); C(7)–C(11) 1.335(9); P–Au–Br(1) 175.98(4).

bered ring is in an envelope conformation with a 19.8° dihedral flap angle.

We could readily brominate dppf and dippf to give the tribromo substituted phosphinocyclopentenes **7** and **8** and were isolated as red oils, in good yields (Scheme 3). However, attempts to complex these brominated phosphinocyclopentenes with [AuCl(tht)] and [PdCl$_2$(NCMe)$_2$] were unsuccessful. This could be due to the reduced donor ability of the phosphorus atom by the bromide atoms on the cyclopentene ring.

It is clear that demetallation resulted from addition of bromine to the cyclopentadienyl moiety and that the coordinated Au metal plays no role in promoting the demetal-

R=Ph **7**, i-Pr **8**

Scheme 3. (i) Bromination in an inert atmosphere and (ii) bromination in air, using moist solvents.

R			R	Yield (%)	
Ph	**3**		Ph	60	**5**
i-Pr	**4**		i-Pr	67	**6**

Scheme 2. Bromination of bis(phosphino)ferrocene gold complexes.

lation. In fact, the intrinsic high nucleophilic character of the aromatic cyclopentadienyl ring makes them more susceptible to electrophilic addition by powerful oxidants such as Br_2 or Cl_2. The halogenation of cyclopentadienyl rings takes place following the same mechanism known for halo-genation of alkenes. This S_N2 like mechanism results in an overall *trans* addition of the halides. The *trans* addition is in good agreement with what is observed in the molecular structure of **6**, where bromines on adjacent carbons are found to be *trans* to each other.
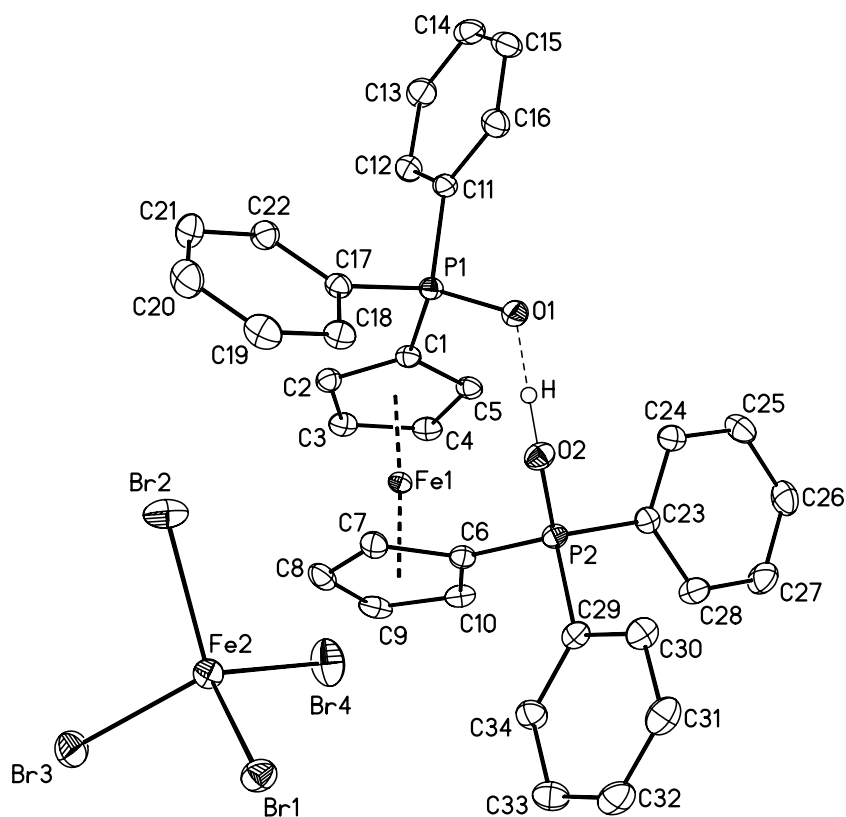
Fig. 5(a). A molecular drawing of **9**. All H atoms except hydroxyl atom H are omitted.
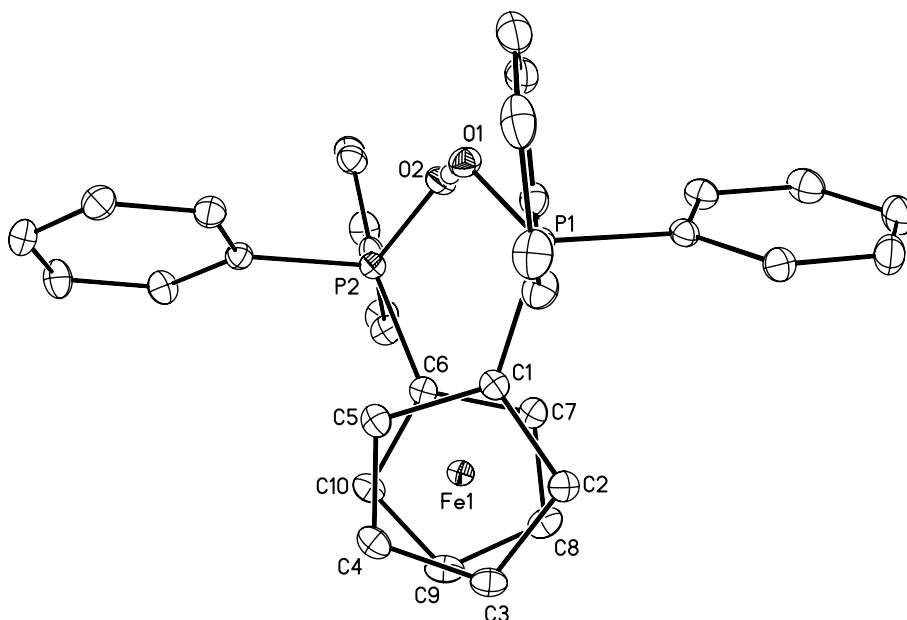
Fig. 5(b). A top view of the structure of **9**. The counterion and all H atoms except the hydroxyl H atom are omitted.

Table 2
Selected bond lengths [Å] and angles [°] for **9**

Bond lengths [Å]	
P(1)–O(1)	1.5229(11)
P(1)–C(1)	1.7697(15)
P(1)–C(11)	1.7899(15)
P(1)–C(17)	1.7935(15)
P(2)–O(2)	1.5257(11)
P(2)–C(6)	1.7701(15)
P(2)–C(29)	1.7864(14)
P(2)–C(23)	1.7969(15)
O(1)–H	1.39(4)
O(2)–H	1.03(4)
Bond angles [°]	
O(1)–P(1)–C(1)	112.60(6)
O(1)–P(1)–C(11)	108.50(7)
C(1)–P(1)–C(11)	105.79(7)
O(1)–P(1)–C(17)	111.36(7)
C(1)–P(1)–C(17)	109.17(7)
C(11)–P(1)–C(17)	109.23(7)
O(2)–P(2)–C(6)	111.05(6)
O(2)–P(2)–C(29)	109.51(6)
C(6)–P(2)–C(29)	106.96(7)
O(2)–P(2)–C(23)	111.40(7)
C(6)–P(2)–C(23)	110.70(7)
C(29)–P(2)–C(23)	107.03(7)
P(1)–O(1)–H	123.5(15)
P(2)–O(2)–H	120(2)

When bromination was performed using dppf in air it produces an oxidized diphosphine, [doppf][FeBr$_4$] (doppf = 1,1′-bis(oxodiphenylphosphino)ferrocene), product as the major product (**9**), and its structure has been established by single X-ray diffraction. Table 1 contains the crystallographic data and Fig. 5 and Table 2 show the molecular structure and the bond parameters, respectively.

Fig. 5(b) is a top view of **9**, which shows that the two cyclopentadienyl rings are staggered as observed in similar compounds [16]. However, this Fe complex is not pseudo-centrosymmetric or anticlinal and the P–Centroid–Centroid–P torsion angle measures 41.9° corresponding to synclinal arrangement. The reason for this conformation is the hydrogen bonding interaction between the oxygen atoms O1 and O2. Neutral ferrocenephosphine oxides have P=O units that are *trans* and centrosymmetric but it appears that on oxidation of diphosphinoferrocene in moist solvent in the presence of bromine, both phosphorus and iron get oxidized and lose this symmetry. The distance between the two Oxygen atoms, O1 and O2, is 2.417 Å, and is similar to the values of 2.411 (4) reported by Razak et al. [17]. This would induce significant steric conflict between these oxygen atoms, a big conflict unless there is an H atom is present between the O atoms which would result in a very strong O–H···O bond. The ferrocene Fe atom is in the +2 oxidation state in this instance, with the overall positive charge of the cation coming from a proton that hydrogen-bonds the oxygen atoms. Further evidence is in the lengths of the P–O bond lengths, which average to 1.523 Å. Allen et al. [18] reported P–O with a delocalized H atom to be 1.513 Å while Razak et al. [17] obtained values between 1.513 and 1.529 Å.

3. Conclusions

It is clear that the conditions under which the bromination reactions are performed are crucial to the type of the products obtained. When bromination and subsequent demetallation occurs, the basicity of the phosphines is so reduced that any attempts to use these brominated phosphines in synthesis should be preceded by the complexation of the desired metal to the diphospinoferrocene before addition of bromine.

4. Experimental

4.1. General considerations

All reactions were carried out under an atmosphere of pre-purified nitrogen unless otherwise indicated. Air- and/or moisture-sensitive materials were handled using standard Schlenk techniques except in the preparation of **9**. Hexane, benzene, toluene, diethyl ether, and tetrahydrofuran were purified by distillation from sodium benzophenone ketyl under a nitrogen atmosphere. All other solvents were of reagent grade and were used without further purification unless oxygen-free solvent was needed; then the solvent was purged with nitrogen for ca. 15 min. Dppf and dippf were prepared using reported procedures [19]. NMR spectra were recorded on a Gemini 2000 instrument (^{1}H at 200 MHz, ^{13}C at 50 MHz). The chemical shifts are reported in δ (ppm) referenced to residual ^{1}H and ^{13}C signals of deuterated chloroform as internal standard. Microanalyses were carried out at the University of Cape Town (South Africa) using a Fisons EA 1108 CHNS elemental analyzer. Mass spectrometry was performed at the University of Stellenbosch (South Africa) on a Waters API Quatro Micro at a cone voltage of 15 kV.

4.2. Synthesis of dppfAu$_2$Cl$_2$ (**1**)

To sodium tetrachloroaurate(III) dihydrate, Na[AuCl$_4$]·2H$_2$O, (0.33 g, 0.90 mmol) dissolved in acetonitrile and 6 drops of water was added dppf (0.50 g, 0.90 mmol) in dichloromethane (20 mL). The orange solution was stirred until it turned yellow with formation of a white precipitate after an hour. The solvent was removed under vacuum to yield a yellow solid. Recrystallization of the yellow solid by slow diffusion of acetonitrile into a dichloromethane solution of **1** at −15 °C afforded X-ray quality single crystals (0.41 g, 45%). ^{1}H NMR (CDCl$_3$): δ 7.45 (m, 20H, PPh$_2$), 4.72 (s, 4H, C$_5$H$_4$), 4.31 (s, 4H, C$_5$H$_4$). ^{31}P{^{1}H}: δ 30.0.

4.3. Synthesis of dippfAu$_2$Cl$_2$ (**2**)

A solution of dippf (0.25 g, 0.55 mmol) in MeOH (15 mL) was added drop-wise for 25 min to a stirred solution containing Na[AuCl$_4$]·2 H$_2$O (0.22 g, 0.50 mmol) and

sodium chloride (1.13 g, 4.00 mmol) in water (20 mL) at 0 °C. A green solid separated immediately. Stirring was continued for 30 min and the solid was filtered, washed with water (20 mL) and re-dissolved in dichloromethane. Recrystallization by slow diffusion of diethyl ether into a dichloromethane solution of **2** at −15 °C gave X-ray quality single crystals (0.15 g, 42%). ^{1}H NMR (CDCl$_3$): δ 4.75 (s, 4H, C$_5$H$_4$), 4.50 (s, 4H, C$_5$H$_4$), 3.59 (m, 4H, P(*i*-Pr)$_2$), 1.25 (m, 24H, P(*i*-Pr)$_2$). ^{13}C{^{1}H} NMR: δ 74.9 (d, C$_5$H$_4$, J_{P-C} = 28.5 Hz), 73.4 (d, C$_5$H$_4$, J_{P-C} = 28.5 Hz), 25.6 (*i*-Pr), 25.1 (*i*-Pr), 19.3 (*i*-Pr). ^{31}P{^{1}H}: δ 50.0. Anal. Calc. for C$_{22}$H$_{36}$Au$_2$Cl$_2$FeP$_2$ · THF: C 28.63, H 3.90. Found: C 28.78, H 3.86%. MS (ESI) *m/z* (%): 847 (M$^+$−Cl, 100).

4.4. Synthesis of dppfAu$_2$Br$_2$ (3)

To a stirred red solution of Na[AuCl$_4$]·2H$_2$O (0.30 g, 0.75 mmol) and NaBr (0.23 g, 2.25 mmol) in a mixture of water–ethanol (8:2 mL) was added drop-wise, over a period of 20 min a solution of dppf (0.42 g, 0.75 mmol) dissolved in dichloromethane (10 mL). The mixture was stirred for 50 min, after which water was mopped from the reaction by the addition of MgSO$_4$. The green solution was filtered and the filtrate evaporated under reduced pressure. The remaining ethanol solution was decanted from the solid that was then re-dissolved in chloroform and precipitated with hexane to yield a brown solid (0.134 g, 16%). Recrystallization of the brown solid by slow diffusion of THF into a dichloromethane solution of **3** at −15 °C afforded X-ray quality single crystals. ^{1}H NMR (CDCl$_3$): δ 7.47 (s, 20H, PPh$_2$), 4.74 (s, 4H, C$_5$H$_4$), 4.31 (s, 4H, C$_5$H$_4$). ^{31}P{^{1}H}: δ 32.0. Anal. Calc. for C$_{34}$H$_{28}$Au$_2$Br$_2$FeP$_2$ · 0.5THF: C 37.76, H 2.90. Found: C 37.82, H 2.50. MS (ESI) *m/z* (%): 1027 (M$^+$−Br, 10).

4.5. Synthesis of dippfAu$_2$Br$_2$ (4)

A solution of dippf (0.23 g, 0.55 mmol) in MeOH (15 mL) was added drop-wise with stirring to a deep red solution of Na[AuCl$_4$]· 2H$_2$O (0.20 g, 0.50 mmol) and NaBr (0.34 g, 3 mmol) in water (15 mL). A brown solid separated and was filtered after 25 min. Recrystallization by slow diffusion of THF into a dichloromethane solution of **3** at room temperature gave X-ray quality single crystals (0.20 g, 37%). ^{1}H NMR (CDCl$_3$): δ 4.75 (s, 4H, C$_5$H$_4$), 4.50 (s, 4H, C$_5$H$_4$), 3.59 (m, 4H, P(*i*-Pr)$_2$), 1.25 (m, 24H, P(*i*Pr)$_2$). ^{13}C{^{1}H} NMR: δ74.8 (d, C$_5$H$_4$, J_{P-C} = 27.3 Hz), 73.4 (d, C$_5$H$_4$, J_{P-C} = 27.6 Hz), 25.8 (*i*-Pr), 24.5 (s, *i*-Pr), 19.4 (*i*-Pr). ^{31}P{^{1}H} NMR: δ 53.0. Anal. Calc. for C$_{22}$H$_{36}$Au$_2$Br$_2$FeP$_2$: C 27.18, H 3.73. Found: C 27.29, H 4.10. MS (ESI) *m/z* (%): 891 (M$^+$−Br, 70).

4.6. Synthesis of C$_5$H$_4$Br$_3$PPh$_2$AuBr (5)

Complex **3** (0.11 g, 0.1 mmol) was dissolved in dichloromethane (10 mL) and solution cooled to 0 °C. To this

solution was added a solution of Br$_2$ (0.096 g, 0.60 mmol, 0.031 mL) in dichloromethane (10 mL), drop-wise *via* a pressure-equalizing funnel. The resultant red solution was stirred for an hour, filtered and the filtrate evaporated to give a red oil (0.098 g, 64%), that solidified under vacuum. ^{1}H NMR (CDCl$_3$): 7.65 (s, 1H, PPh$_2$), 6.76 (s, 1H, C$_5$H$_4$Br$_3$), 5.77 (s, 1H, C$_5$H$_4$Br$_3$), 5.38 (d, 1H, C$_5$H$_4$Br$_3$, $^3J_{H-H}$ = 16.6 Hz), 5.05 (s,1H, C$_5$H$_4$Br$_3$). ^{31}P{^{1}H}: δ 21.0.

4.7. Synthesis of C$_5$H$_4$Br$_3$P(^{i}Pr)$_2$AuBr (6)

Complex **6** was prepared by a similar procedure as described for **5** using **4** (0.097 g, 0.1 mmol) and Br$_2$ (0.096 g, 0.60 mmol, 0.031 mL). The oil obtained was then re-dissolved in dichloromethane and layered with an equivalent amount of diethyl ether followed by a large excess of hexane and allowed to stand for 3 days. The product was obtained as golden crystals (0.061 g, 44%) suitable for X-ray diffraction studies. ^{1}H NMR (CDCl$_3$): 6.78 (dd, 1H, C$_5$H$_4$Br$_3$, $^3J_{H-H}$ = 0.8 Hz, $^3J_{H-H}$ = 5.8 Hz), 5.25 (d, 1H, C$_5$H$_4$Br$_3$, $^3J_{H-H}$ = 3.0 Hz), 5.20 (d, 1H, C$_5$H$_4$Br$_3$, $^3J_{H-H}$ = 2.2 Hz), 4.98 (t, 1H, C$_5$H$_4$ Br$_3$, $^3J_{H-H}$ = 1.6 Hz), 2.62–2.41 (m, 2H, P(*i*-Pr)$_2$), 1.56–1.18 (m, 12H, P(*i*-Pr)$_2$). ^{13}C {^{1}H}NMR: δ 148 (d, C$_5$H$_4$Br$_3$, J_{P-C} = 29.4 Hz), 131.3 (s, *i*-Pr) 129.2 (s, *i*-Pr), 57.8 (d, C$_5$H$_4$Br$_3$, J_{P-C} = 44.4 Hz), 54.8 (d, C$_5$H$_4$Br$_3$, J_{P-C} = 20.7 Hz), 52.6 (d, C$_5$H$_4$Br$_3$, J_{P-C} = 44.4 Hz), 19.5 (*i*-Pr). 18.7 (*i*-Pr). ^{31}P{^{1}H} NMR: δ 46.0. Anal. Calc. for C$_{11}$H$_{18}$AuBr$_4$P: C 18.93, H 2.60. Found: C 19.05, H 2.55.

4.8. Synthesis of C$_5$H$_4$Br$_3$PPh$_2$ (7)

To an orange solution of dppf (0.20 g, 0.36 mmol) dissolved in dichloromethane (10 mL) and cooled to 0 °C, a solution of Br$_2$ (0.35 g, 2.16 mmol) dissolved in dichloromethane (15 mL) was added drop-wise *via* a pressure-equalizing dropping funnel. The resulting deep red solution was stirred for an hour, filtered and concentrated and ether (10 mL) was added. The product was obtained as red wax (0.21 g, 60%). ^{1}H NMR (CDCl$_3$): 7.64 (s, 1H, C$_5$H$_4$Br$_3$), 7.47 (m, 10H, PPh$_2$), 4.27 (s, 1H, C$_5$H$_4$Br$_3$), 4.25 (s, 1H, C$_5$H$_4$Br$_3$). ^{31}P{^{1}H} NMR: δ 28.0.

4.9. Synthesis of C$_5$H$_4$Br$_3$P(^{i}Pr)$_2$ (8)

Compound **8** was prepared in a similar manner to **7** using dippf (0.20 g, 0.48 mmol) and Br$_2$. The resulting deep red solution was stirred for an hour, filtered and evaporated. The crude product was then purified by column chromatography over silica using a mixture of dichloromethane and hexane as eluent (1:2). The product was obtained as red oil (0.27 g, 67%). ^{1}H NMR (CDCl$_3$): 7.73 (s, 1H, C$_5$H$_4$Br$_3$), 7.57 (s, 1H, C$_5$H$_4$Br$_3$), 4.25 (s,1H, C$_5$H$_4$Br$_3$), 4.24 (s,1H, C$_5$H$_4$Br$_3$), 3.02 (s, 2H, P(*i*-Pr$_2$)$_2$), 1.36 (s, 6H, P(*i*-Pr$_2$)$_2$). ^{31}P{^{1}H}: δ 35.0.

4.10. Synthesis of doppfFeBr$_4$ (**9**)

To an orange solution of dppf (0.28 g, 0.50 mmol) dissolved in dichloromethane (10 mL) and cooled to 0 °C, a solution of Br$_2$ (0.48 g, 3.0 mmol) dissolved in dichloromethane (15 mL) was added drop-wise *via* a pressure-equalizing funnel. The resulting deep red solution was stirred for an hour, filtered and evaporated to afford a red solid. Recrystallization from chloroform gave red crystals (0.27 g, 56%), suitable for X-ray diffraction studies. ^{31}P{^{1}H}: δ 28.0. IR (nujol mull): υ(P=O)1168 cm^{-1}. MS (ESI): *m/z* (%) 587 (M$^+$−FeBr$_4$, 100).

4.11. X-ray structural determination

Crystal evaluation and data collection were performed on a Bruker CCD-1000 diffractometer with Mo Kα ($\lambda = 0.71073$ Å) radiation and the diffractometer to crystal distance of 4.9 cm. The initial cell constants were obtained from three series of *w* scans at different starting angles. The reflections were successfully indexed by an automated indexing routine built in the SMART program. These highly redundant data sets were corrected for Lorentz and polarization effects. The absorption correction was based on fitting a function to the empirical transmission surface as sampled by multiple equivalent measurements [20]. A successful solution by the direct methods provided most non-hydrogen atoms from the *E*-map. The remaining non-hydrogen atoms were located in an alternating series of least-squares cycles and difference Fourier maps. All non-hydrogen atoms were refined with anisotropic displacement coefficients. All hydrogen atoms were included in the structure factor calculation at idealized positions and were allowed to ride on the neighbouring atoms with relative isotropic displacement coefficients.

Acknowledgements

Appendix A. Supplementary data

CCDC 665047, 665048, 665049, 665050 and 665051 contain the supplementary crystallographic data for this paper. These data can be obtained free of charge from The Cambridge Crystallographic Data Centre via www.ccdc.cam.ac.uk/data_request/cif. Supplementary data associated with this article can be found, in the online version, at doi:10.1016/j.jorganchem.2007.11.057.

References

[1] A. Togni, T. Hayashi, Ferrocenes: homogeneous catalysisOrganic Synthesis and Materials Science, Wiley, New York, 1995.
[2] N.J. Long, Angew. Chem., Int. Ed. Engl. 34 (1995) 21.
[3] A. Togni, R.L. Halterman, Metallocenes: Synthesis, Reactivity, Applications, Wiley, New York, 1998.
[4] N.J. Long, Metallocenes: An Introduction to Sandwich Complexes, Blackwell Science, Oxford, 1998.
[5] G. Bandoli, A. Dolmella, Coord. Chem. Rev. 209 (2000) 161.
[6] L. Maisela, M.Sc. Dissertation, University of the Western Cape, 2000.
[7] M.C. Gimeno, A. Laguna, C. Sarroca, Inorg. Chem. 32 (1993) 5926.
[8] F. Carioti, L. Naldini, G. Simonetta, Q. Malatesto, Inorg. Chim. Acta 1 (1967) 315.
[9] (a) O. Crespo, M.C. Gimeno, P.G. Jones, A. Laguna, Acta Crystallogr., Sect. C: Cryst. Struct. Commun. 56 (2000) 1433;
(b) Z.A. Sam, A. Oskarsson, S.K.C. Elmroth, A. Roodt, Acta Crystallogr. Sect. E: Struc. Rep. 61 (2005) o2090 (online).
[10] D.T. Hill, G.R. Girard, F.L. McCabe, R.K. Johnson, P.D. Stupik, J.H. Zhang, W.M. Reiff, D.S. Eggleston, Inorg. Chem. 28 (1989) 3529.
[11] F. Canales, M.C. Gimeno, P.G. Jones, A. Laguna, C. Sarroca, Inorg. Chem. 36 (1997) 5206.
[12] J.H.L. Ong, C. Nataro, J.A. Golen, A.L. Rheingold, Organometallics 22 (2003) 5027.
[13] (a) C. Loubser, C. Imrie, P.H. van Rooyen, Adv. Mater. 5 (1993) 45;
(b) R.M.G. Roberts, J. Silver, B.M. Yamin, M.G.B. Drew, U. Eberhardt, J. Chem. Soc., Dalton Trans. (1988) 1549.
[14] D. Schneider, A. Schier, H. Schmidbaur, Dalton Trans. (2004) 1995–2005.
[15] B.M. Wile, R. McDonald, M.J. Ferguson, M. Stradiotto, Organometallics 26 (2007) 1069.
[16] (a) G. Pilloni, B. Corain, M. Degano, B. Longato, G. Zanotti, J. Chem. Soc., Dalton Trans. (1993) 1777;
(b) V. Munyejabo, M. Postel, J.L. Roustan, C. Bensimon, Acta Crystallogr. 50 (1994) 224.
[17] I.A. Razak, A. Usman, H.-K. Fun, B.M. Yamin, N.A.M. Kasim, Acta Crystallogr. Sect. C: Cryst. Struc. Commun. 58 (2002) 225.
[18] F.H. Allen, O. Kennard, D.G. Watson, L. Brammer, A.G. Orpen, R. Taylor, J. Chem. Soc., Perkin Trans. (1987) S1.
[19] J.J. Bishop, A. Davidson, M.L. Katscher, D.W. Lichtenberg, R.E. Merril, J.C. Smart, J. Organomet. Chem. 27 (1971) 241.
[20] Bruker-AXS (2000–2003), SADABS V.2.05, SAINT V.6.22, SHELXTL V.6.10, SMART 5.622 Software Reference Manuals, Bruker-AXS, Madison, WI, USA.